Nonuniformity of Tumor Dose in Radioimmunotherapy

J. L. Humm and L. M. Cobb

Cancer Research Campaign Laboratories, Department of Medical Oncology, Charing Cross Hospital, London, UK; and Division of Experimental, Pathology and Therapeutics, MRC Radiobiology Unit, Harwell, Didcot, UK

The conventional approach to calculating tumor radiation dose from internally administered radioisotopes is by the MIRD schema. The raw input data for such dose calculations is obtained by immunoscintigraphic methods, PLANAR or SPECT imaging. Limitations in the spatial resolution of these techniques can lead to a considerable underestimate of the gross variation in tumor dose. The use of radiolabeled monoclonal antibodies for therapy can result in large nonuniformities in tumor dose. This paper discusses how antibody distribution can influence the energy deposition in the nuclei of target cells. Heterogeneity of antibody binding will lead to an expected decrease in the effectiveness of the radiation delivered. However, enhanced cell killing is possible if the radiolabeled Ab binds to the cell surface membrane and may be further enhanced if the Ab is internalized. Calculations are presented for two cases: (a) a three-dimensional random packing arrangement of cells as a model of the astructural nondifferentiated form seen in some tumors, and (b) differentiated carcinoma of the colon with the cells in tubules. Results for the magnitude of the mean energy deposition to individual cell nuclei from: (a) cell membrane bound ^{211}At, ^{199}Au, ^{131}I, and ^{90}Y-labeled Abs, and (b) a uniform distribution of these sources, as a function of internuclear distance for the two histologies are presented. Energy deposition in tumor cell nuclei from membrane bound radiolabeled antibody may be several times greater than estimated with the assumption of a uniform source distribution.

J Nucl Med 1990; 31:75–83

The use of antibodies (Ab) to target therapeutic amounts of radionuclides to tumors (radioimmunotherapy; RIT) is receiving increasing attention. Initial clinical trials have produced some encouraging results (*1–3*), but there are clearly difficulties. Amongst these are the poor uptake ratio of Ab in tumor versus sensitive normal tissues (*4–5*) and immunological reaction of the patient against the Ab (*6–7*). Compounding these problems is the lack of detailed knowledge of the radiation dosimetry in the tumor, and hence of the appropriate amount of labeled Ab required for a therapeutic effect. This is a complex area made worse by a lack of knowledge of the microdistribution of the source of ionizing radiations (antibody-radionuclide conjugate) and the sites of the relevant target cells (tumor stem-cells).

Heterogeneity of intratumor distribution of injected Ab has a number of causes, some of which have recently been discussed and reviewed (*8–9*). The histology of malignancy reveals that the distribution of tumor cells within a tumor mass is not homogeneous. Single cells or small groups of cells may be separated by large volumes of host-reaction or tumor secretion with the tumor cells constituting only a few percent of the tumor mass. Superimposed upon this irregular distribution of cells can be an equally irregular expression of the antigen to which the Ab is directed (*10–11*). Furthermore, the targeted antigen may be shed from the tumor cells and spread irregularly in the tumor. Immunohistochemistry of sections of breast and colon can show concentrations of carcinoembryonic antigen (CEA) in pools of cell secretion. Ultrastructural studies of tumor blood vessels show irregular patterns of intercellular gaps, endothelial cell fenestration and basement membrane structure which point to a great variation in the permeability of these vessels to Ab (*12*). Once the Ab has exited from the vessels and passed through the subendothelial basement membrane, its distribution will in part be dictated by the kinetics of Ab binding to antigen, particularly that adjacent to the blood vessels (*13*). Finally, the tumor cells may be firmly "cemented" to each other in "nests" from which the large Ab molecule is excluded. The above factors serve to prevent homogeneous distribution of Ab in a tumor mass. In addition, it can be expected that the tidal movement of Ab into and out of a tumor with time, partly reflecting circulatory levels, will greatly complicate the dosimetry. In normal tissues the lymphatic vessels drain away extravasated Ab; but lymphatic drainage is virtually nonexistent in tumors and therefore the Ab seeps back into the circulation in a haphazard manner.

The cells in which our interest is focused are the stem cells, both the cells which under normal circumstances maintain and expand the tumor mass by repeated division, and those which under changing conditions in

Received May 15, 1989; revision accepted Sept. 13, 1989.

For reprints contact: J.L. Humm, PhD, Joint Center for Radiation Therapy and Dept. of Radiation Therapy, Harvard Medical School, 50 Binney St., Boston MA 02115.

the tumor may be stimulated to do so. The stem cell percentage in transplantable animal tumors is commonly as high as 100% (*14*). On the other hand, in man, in vitro assays reveal a stem cell population in the order of 0.1% (*15*).

The purpose of this paper is to explore the implications of the distribution of radiolabeled Ab in the tumor on the microdosimetry, i.e., the energy deposition at the cellular level. This paper will present calculations of the energy deposition from Ab radiolabeled with: astatine-211 (^{211}At), gold-199 (^{199}Au), iodine-131 (^{131}I), and yttrium-90 (^{90}Y). The implications of tumor histology on the energy deposition from bound radiolabeled Ab will be discussed using the example of an adenocarcinoma with its tubular structure as is commonly seen in differentiated colorectal carcinomas.

METHOD

Choice of Radionuclide

The radionuclides that have been used in clinical radioimmunotherapy thus far are ^{131}I (*16–19*) and ^{90}Y (*20–21*). There is still much debate as to the best isotope for RIT. Both the above sources have disadvantages: ^{131}I releases two-thirds of its energy as penetrating gamma-radiation, much of which will be dissipated in normal tissues surrounding the tumor, and ^{90}Y is a pure beta-emitter which will go to bone and hence irradiate bone marrow, if it becomes detached from the Ab chelate (*22*). In this paper results will be shown for both these isotopes as well as for the alpha-source ^{211}At, which has shown promising results in animal studies (*23*), and for the short range beta-source ^{199}Au.

Dosimetry and Microdosimetry

The traditional procedure for evaluating the radiation dose from internally administered radionuclides to any tissue or organ is described in the ICRU report 32 (*24*). The method consists of the evaluation of the dose to the target organ from two components: (a) the sources incorporated within the target tissue and (b) sources in adjacent tissues. The first component is based on the assumption that the distribution of sources within the target is uniform and involves the evaluation of the total energy released from source decays in the target volume corrected for the escaping fraction. The second component, which applies usually only to photon radiations, is based on the work of Snyder et al. (*25*) who have produced tables of S values, that are calculated values of the absorbed fraction in one organ from a homogeneous distribution of monoenergetic gamma-emissions from other individual organs, for a model human body designed to be close to those of standard man (*26*) and reference man (*27*). This work was later extended by Snyder (*28*) for several of the radionuclides listed in Dillman and Van der Lage (*29*).

This approach has severe limitations when applied to RIT where the targeted radionuclide may exhibit considerable spatial and temporal variations. The aim of RIT is to sterilize all tumor stem cells, or where they are not identifiable all tumor cells. Therefore a more detailed knowledge of the variation in dose at a cellular level will lead to a rationale for the optimization of RIT. In addition to problems of the MIRD formulation posed by Ab heterogeneity in the tumor is the influence of Ab binding and possibly internalization, on the dose to the relevant tumor cells. The Medical Internal Radiation Dose Committee (MIRD) approach does not distinguish between a uniform distribution of nonspecific radiolabeled Ab and one that binds uniformly to cell surface antigen; the nominal tumor doses would be considered identical given the same relative specific activities in the two cases. However, if the DNA is the predominant target for cell inactivation at therapeutic doses, rather than the dose to the tissue as a whole, the dose to the cell nuclei would be a more appropriate quantity to correlate with tumor cell sterilization. The mean dose to cell nuclei from radiolabeled Ab bound to cell surface antigen may differ considerably from the nuclear dose from radiolabeled Ab distributed uniformly in the tissue space as shown later. To determine the enhanced dose to tumor cell nuclei as a result of Ab binding to cell surface antigen requires a microdosimetric approach.

Homogeneous Ab distribution is not found in practice and therefore the concept of a single dose value for a tumor can only have limited value. While heterogeneity of Ab within tumors is of less concern in radioimmunoscintigraphy (only the tumor/background ratios are important for detection) it may have profound implications for RIT. If the selection of a radionuclide for RIT with a short range emission is to be preferred on account of obtaining higher tumor/non-tumor dose ratios (*30*), then the magnitude of distances across areas of poor Ab localization, "cold regions", will have considerable bearing on how short the emission path lengths can be for an efficacious therapy. As a working hypothesis the optimum radionuclide for RIT would be one in which the mean range is approximately equal to the diameter of the largest "cold region" in the tumor. In practice information on cold-regions is not known and would be exceedingly difficult to obtain.

Some of the questions arising from heterogeneous beta-source distributions which could be described analytically have been treated before (*31–33*). A technique for measuring variations in tumor dose using miniature TLD implants has been developed by Wessels and colleagues (*34–35*). However these studies do not discuss energy deposition at the cellular and sub-cellular level. Fisher (*36*) was the first to a apply a microdosimetric analysis for the case of alpha-emitters to RIT. The aim of this paper is to develop some of these microdosimetric ideas further.

Dose Across "Cold-Regions"

Calculations to estimate the dose across cold regions have been performed by Humm (*30*) who obtained the dose gradient, expressed as a fraction of the MIRD dose, across a spherical cold region devoid of radiolabeled Ab surrounded by a uniform distribution of radiolabeled Ab of thickness greater than R_{max} which is the range of the most energetic beta-particle emitted. Illustrations of dose profiles for ^{90}Y, ^{77}As and ^{199}Au, beta-emitters of quite different ranges, across cold-regions of 0.5, 1, 2 and 4 mm radii, given in Humm (*30*) show that gross heterogeneities in spatial distribution of Ab favor the choice of longer range beta-emitters.

Dose at the Cellular Level

The radiosensitivity of a population of tumor cells is often expressed by the D_0 (the inverse slope of the linear portion of the survival curve). For alpha-particles with linear survival

curves and known D_0 the dose required to reduce the cell population to any level of cell survival can be extrapolated from the equation

$$D = - D_0 \ln S, \quad (1)$$

e.g., $D = 4.605D_0$ is the dose to reduce a population to a fraction of 0.01 survivors. Typical D_0 values for alpha-particles range between 0.5–1.0 Gy (*37–38*) depending on the cell line. Taking a D_0 value of 0.7 Gy gives from Equation (1) D = 3.22 Gy for 99% cell sterilization. Mammalian cell survival curves for beta-particles are shouldered, the shoulder width varying for different cell lines. At the 0.01 survival level the relative biological effectiveness (α/β particles) is typically ~3 although it varies considerably with dose rate reaching values as great as 10 at low dose rates (*39*).

A radiolabeled Ab which is present in the tumor when the source decays, releases a particle which traverses the tumor mass depositing energy along its path. Some of the energy is deposited in the extra-cellular volume V_e, some in the volume occupied by the cell cytoplasm V_c and some in the cell nuclei V_n. The mean fraction of energy deposited in each, from a large number of decays positioned at random, is given by the ratio of each respective volume relative to the total tissue volume V_t. For a fixed number of decays the amount of energy deposition in the cell nuclei therefore depends on the density of the nuclear packing in the tumor. This will vary between tumor types and may vary from one region in a tumor to another. If the source disintegrations occur truly at random within the tumor then the average dose to the cell nuclei, cell and total tissue volumes are identical. For example, if the cell nuclei constitute 10% of the total volume, i.e., $V_n/V_t = 0.1$, then only 10% of the total energy deposited in the tissue will be in cell nuclei. This nuclear volume fraction (V_n/V_t) will be called V_v.

If the sources are not truly uniformly distributed, but localized to the surface of the tumor cell membrane, then the dose to the cell nuclei may not be in equilibrium with the tissue. The mean energy deposition to cell nuclei ϵ has been calculated for a diverse range of potentially useful isotopes for RIT: ^{211}At, ^{199}Au, ^{131}I, and ^{90}Y, for the case of a uniform distribution of cell surface bound radiolabeled Ab and for a uniform source distribution (Fig. 1). Calculations have been performed for spherical cells of 7 μm and 10 μm radii with isocentric nuclei of 3.5 μm and 5 μm radii respectively and for internuclear spacings from 7 μm to 100 μm. For a random decay in which it is assumed that the entire track lies within the tumor, the mean energy deposited in cell nuclei per decay ϵ_{MIRD} is the product of the particle energy E and the nuclear volume fraction

$$\epsilon_{MIRD} = E * V_v. \quad (2)$$

Table 1 gives the calculated energy deposition in nuclei with radii 5 μm per disintegration. Note that the mean dose to the tumor cell nuclei is equal to the tissue dose, expected from the conditions of the MIRD equation.

When the radiolabeled Ab binds to cell surface antigen the above expression has to be modified to account for the bias resulting from the geometric localizing of the source to the target nuclei. The dose to the nuclear volume fraction may now be expressed as the sum of two components: the energy deposition to the cell nucleus from sources bound to the cell membrane of that cell ϵ_{SELF} and the nonspecific or nontargetted energy deposition ϵ_{NEIGH} to all neighbouring cell nuclei to which the source is not bound. The energy deposition to all neighbouring nuclei ϵ_{NEIGH} is given by Equation (3),

$$\epsilon_{NEIGH} = E * V'_v, \quad (3)$$

where V'_v is a modified volume fraction to include the reduction in the overlap of the particle track with the nuclei due to biasing the decay site to points exterior to the cell. For internuclear distances >30 μm V'_v is equal to V_v to within 1%, since the nuclear volume fraction is negligible. This agreement is also valid for ^{90}Y (mean range 3960 μm) up to the highest cell densities since with long range emissions many nuclei are intersected and source biasing only affects the overlap of the particle track with the closest cell nucleus. For the short range, ^{211}At emission (60 μm) any biasing in the source location involves a considerable fraction (0.2) of the particle range.

Added to the component described by Equation (3) is the energy deposition to the cell nucleus to which the Ab is bound. This additional energy deposition ϵ_{SELF} is given by Equation (4):

$$\epsilon_{SELF} = p * l * \sum (f * LET)_i, \quad (4)$$

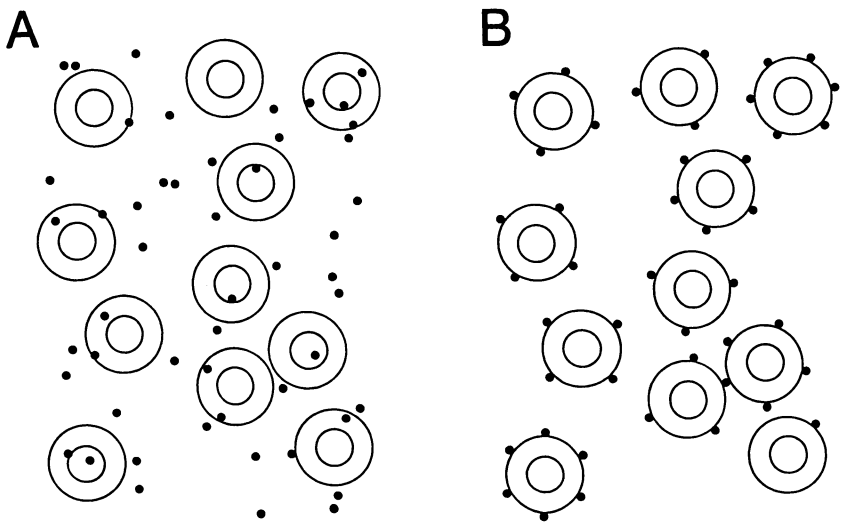

FIGURE 1
A random distribution of cells with two different source distributions of the same relative specific activity superimposed upon it: (A) sources are distributed uniformly (MIRD case), and (B) sources are geometrically placed on the cell membrane.

TABLE 1
Mean Energy Deposition per Cell Nucleus per Source Disintegration for a Random Decay Site as a Function of Mean Internuclear Distance*

Internuclear distance (μm)	Mean energy per decay (keV)	Energy deposited per nucleus per decay (keV)				
		10	20	30	50	100
^{211}At	6767	511	63.9	18.9	4.09	0.511
^{199}Au	143	10.81	1.35	0.40	0.086	0.0108
^{131}I	190	14.36	1.80	0.53	0.115	0.0144
^{90}Y	935	70.66	8.83	2.62	0.565	0.0707

* Cell and nuclei are assumed to be isocentric spheres of 10 μm and 5 μm radius, respectively.

where p is the probability of a nuclear traversal and depends on the solid angle of the nucleus subtended by a point on the cell membrane, $\bar{l}$ is the mean path length across the nucleus and $\sum (f * LET)_i$ is the sum of the linear energy transfers for each component i, with f emissions per transformation, in the decay scheme. For spherical cells and nuclei $p = \omega/4\prod$ where $\omega = 0.268\prod$ steradians when the cell radius x is twice the radius a of the nucleus i.e. both x = 10 μm and a = 5 μm as well as x = 7 μm and a = 3.5 μm. The value of $\bar{l}$ is given by

$$\bar{l} = \frac{1}{2\,(x-(x^2-a^2)^{0.5})} \cdot (2ax-(x^2-a^2)\frac{\ln(x+a)}{(x-a)}), \qquad (5)$$

which for the nuclear radii 3.5 μm and 5 μm gives 4.663 μm and 6.663 μm, respectively. For radionuclides which emit one particle per decay, e.g., ^{90}Y, a mean LET for the relevant segment of the particle track should be used, not the track averaged LET, so as not to overestimate the energy deposition. Many beta-sources also have additional emissions from internal conversion and Auger electrons. Those with energies sufficient to reach the cell nucleus should also be considered in the analysis. The sum of Equations (3) and (4) gives the energy deposition, ϵ_{bound}, for the case of membrane bound Ab. Values for ϵ_{MIRD} and ϵ_{bound} are given in Table 2. The sum of Equation (3) and (4) divided by Equation (2) yields Equation (6) which is the enhanced energy deposition G due to the geometric localization of the source to the cell membrane.

$$G = \frac{E * V' + p * \bar{l} * \sum (f * LET)_i}{E * V_v} \qquad (6)$$

Since usually $V'_v = V_v$ Equation (6) simplifies to

$$G = 1 + \frac{p * \bar{l} * \sum (f * LET)_i}{E * V_v}. \qquad (7)$$

Note that the enhancements arise solely as a result of the geometric biasing of the site of the radionuclide decay and therefore are geometric enhancement factors. Values for Equation (7) are given in Table 3 and Table 4 for nuclei of radii 5 μm and 3.5 μm, respectively. Note that the emission of more than one particle per disintegration, i.e., the emission of internal conversion and/or KXY Auger electrons produces an increase in the geometric enhancement factors.

Where the cells are packed closely in a tumor the deviation from the MIRD calculations is small even for the short range sources. The magnitude of the deviation increases rapidly with increasing inter-nuclear distances between nearest neighbors. This is because the nuclear volume fraction V_v is related to the inter-nuclear distance by the inverse cube, so that at inter edge to edge nuclear distances greater than about one tenth of the particle range, the fraction of the particle energy deposited in the nuclear volume, (i.e., the magnitude of crossfire) becomes much smaller than the contribution due to binding. The geometric enhancement (due to membrane bound Ab) occurring with the short range alpha- and beta-sources can be enormous at internuclear spacing quite realistic for many tumors. These results do not take into account the likely situation of a proportion of the Ab binding to non-cell-surface antigens, internalized Ab (which would magnify the effect even more if loss of the radionuclide does not occur) or the heterogeneity of Ab binding which leads to further complications in the interpretation of absorbed dose. Note that Equation (7) is not valid for emitters of particles with ranges insufficient to fully traverse or even reach the cell nucleus when bound to cell surface antigen. Such may be the case with some Auger sources, when enhancements <1 may result, i.e., the energy deposition to the nucleus is greater for a uniform distribution of sources than for source decays on the

TABLE 2
Sources located on the outer cell membrane*

Internuclear distance (μm)	Mean energy per decay (keV)	Energy deposited per nucleus per decay (keV)				
		10	20	30	50	100
^{211}At	6767	547	99.4	54.4	39.4	36.0
^{199}Au	143 × 1.42	12.18	1.48	0.53	0.212	0.137
^{131}I	190 × 1.06	15.31	2.00	0.66	0.216	0.109
^{90}Y	935	70.75	8.921	2.71	0.654	0.160

* The multiplicative factors 1.42 and 1.06 denote the additional electron energy deposition component due to internal conversion.

TABLE 3
Geometric Enhancement Factors, i.e., the Corresponding Values from Table 2 (Membrane Bound Radiolabeled Ab) Divided by Those of Table 1 (Uniform Source Distribution) as a Function of Internuclear Distance*

Internuclear distance (μm)	Geometric enhancement factors				
	10	20	30	50	100
^{211}At	1.07	1.56	2.88	9.69	70.5
^{199}Au	1.01	1.09	1.32	2.47	12.67
^{131}I	1.006	1.05	1.17	1.77	7.17
^{90}Y	1.001	1.01	1.034	1.16	2.26

* Cells are spheres of radius 10 μm containing isocentric spherical nuclei of 5 μm radius.

cell surface. This effect has been reported in the context of boron capture therapy by Gabel et al. (*40*). It should be further noted that the MIRD uniform source distribution and the case of radiolabeled nonspecific Ab are different. Non-specific Ab will often be uniformly distributed only extra-cellularly, and hence the MIRD dose approach will result in an overestimation of the mean dose experienced by an assembly of tumor cell nuclei.

The values presented in Table 2 can be used to calculate the number of source disintegrations required per cell at the surface membrane for a required level of cell sterilization, assuming uniform Ab binding on the surface. If the dose required for 99% cell inactivation equals $4.605D_0$, then dividing this value by the mean nuclear dose per source decay (obtained from Table 2) yields the number of decays per cell for the desired level of cell sterilization. Figures are presented in Table 5 for 99% inactivation which can easily be adjusted for any level of cell killing. These values give the actual number of disintegrations required and not the number of Abs. To relate to the number of Abs required per cell these numbers need to be adjusted for the radiolabeling efficiency and the retention time of the Ab on the cell surface in relation to the radionuclide half-life. Furthermore, for the beta-emitters adjustments have to be made for the oxygen status of the cells and the dose rate. The D_0 assumed here for beta-particles, 2.1Gy, is typical of an acute dose rate and for well-oxygenated tissue. Therefore the numbers in Table 5 require further modification to take into account low dose rate effects and oxygen status.

Monte-Carlo Approach to Microdosimetry of Radiolabeled Antibodies

A Monte-Carlo computer model to calculate the energy deposition to individual tumor cell nuclei following the administration of ^{211}At radiolabeled Abs has been described by Humm (*41*). The results presented in that study discussed two extreme cases (a) when the radiolabeled Ab remained in the blood stream; and (b) for a uniform distribution of sources in the tumor. The model assumed for the tumor was a simple random packing of tumor cell nuclei. This model has been extended in this paper to simulate the tubular structure typical of differentiated colorectal carcinomas as illustrated in Figure 2. Cells of 10 μm radii containing 5 μm spherical cell nuclei are assumed to be packed along the cylinders which are

TABLE 4
Cell and Nuclei of Radius 7 μm and 3.5 μm, respectively

Internuclear distance (μm)	Geometric enhancement factors					
	7	10	20	30	50	100
^{211}At	1.07	1.20	2.62	6.48	26.3	204
^{199}Au	1.01	1.03	1.27	1.92	5.27	35
^{131}I	1.007	1.02	1.15	1.52	3.39	20
^{90}Y	1.001	1.004	1.03	1.10	1.46	4.7

separated by a variable distance c. The sources (^{211}At or ^{131}I) are placed on the outer surfaces of the cylinders. For ^{211}At both the direct 5.87 MeV alpha-particle and the 7.45 MeV alpha from the polonium-211 (^{211}Po) daughter are considered; the ranges are 50 μm and 67 μm, respectively. For a given concentration of sources each radionuclide decay is simulated by choosing a random emission direction and the intersection coordinates calculated for every traversed cell nucleus. The energy deposition resulting from each alpha-traversal is obtained from the difference in residual energy between entrance and exit of the nucleus. Tracks which terminate in a nucleus deposit an energy equal to the residual energy of the alpha-particle upon entering the nucleus. The residual alpha-energy at each nuclear intersection is interpolated from the experimental values for α-particles in soft tissue by Walsh (*42*). A microdosimetric spectrum of energy deposition is obtained by summing the energy deposition to each cell nucleus for the desired number of decays.

For ^{131}I disintegrations a simple constant LET (0.2 keV/μm) model is used in which straight line tracks are assumed of range 487 μm, equivalent to the mean range of the beta-spectrum (note that this is not the same as the range of the mean beta-energy).

RESULTS

For the cylindrical geometry of Figure 2 there is an effect similar to the enhancement shown in Tables 3 and 4. Suppose there is a given number of decays per

TABLE 5
Number of Source Decays at the Cell Membrane, per Cell, for 99% Cell inactivation*

internuclear distance (μm)	No. of source decays per cell for 99% Inactivation				
	10	20	30	50	100
^{211}At	19.3	106	194	266	293
^{199}Au	2597	21419	60145	149229	230923
^{131}I	2066	15842	48080	146465	289446
^{90}Y	447	3546	11691	48374	198348

* The D_0 values assumed in this work were 0.7 and 2.1 Gy for alpha- and beta-particles, respectively. To adjust the table values for 99.9% inactivation multiply required source number by 1.5, for 99.99% inactivation multiply source number by 2.0, for 99.999 multiply by 2.5, etc. These data are for cell and nuclear radii of 10 μm and 5 μm, respectively.

cell in the tumor. If all these disintegrations occur randomly within the tissue one obtains a dose to the nuclei D_{MIRD} which is equal to the MIRD dose. If the same number of decays occur on the outer surface of the tubules (Fig. 2), as might be the case for radiolabeled Ab binding to available antigen expressed on this surface, one obtains typically a larger nuclear dose D_{bound}. Values are obtained for the mean energy deposition per cell nucleus expressed per source decay for a uniform distribution of unbound and bound (to the outer tubular surface) sources for several inter-tubule spacings c (Table 6). These values are plotted in Figure 3. The ratio of these curves gives the geometric enhancement factor D_{bound}/D_{MIRD} shown in Table 6. Note that the enhancement factor decreases slightly for small inter-tubular spacing. This effect arises because the sources are moved from a random placement within the tumor volume to positions only on the outer surfaces of the tubules. This rearrangement means that sources from within the tubule (within radius b/2), which contribute significantly to the nuclear dose are excluded from geometric locations which are heavily weighted to deposit energy within the nuclear regions. As the inter-tubule distance c increases, the number of source decays within a tubule falls in proportion to the intra-tubule volume fraction. As the fraction of intra-tubule sources approaches zero then the enhancement factor rapidly increases approaching in the limit c^2. If sources are excluded from the intra-tubule volume in the random decay site calculations, then the enhancement factor does not exhibit a decrease for small inter-tubule spacing (this is perhaps a more appropriate model for a non-specific Ab than the strict MIRD uniform distribution). Note that the geometric enhancement value for this tubular histology increases as the square of the inter-tubule spacing c, much slower than for a random arrangement of isolated cells which increases in the limit as the cube of the inter-nuclear distance. This results from the assumed infinite cylindrical geometry so that the source volume dilution falls ultimately as $1/c^2$.

For ^{211}At the calculations were performed for both constant LET energy loss and according to the Bragg curve. The enhancement value for tightly packed tubules differs by only 1% for the two energy loss models, when the outer surfaces of the cylinders are in contact (each cylinder possessing six neighbors) G = 1.48 and 1.47. For ^{131}I G = 1.29, a value much lower than for ^{211}At as the result of the higher cross-fire component from sources attached to cylinders more distant than the six nearest neighbors. For inter-cylinder distances <50 μm the fall in energy deposition for both source configurations is similar, therefore the variation in enhancement due to binding is small. As the cylinder spacing increases beyond 50 μm the fall in energy deposition due to random source placement declines increasingly more rapidly than for bound radionuclide, hence the increasing rise in enhancement factors. For ^{131}I at mean inter-tubular distances of 200 μm G = 2, whereas for ^{211}At it already approaches 6. There is autoradiographic evidence with colorectal xenograft models and patients (*43*, Begent R.: private communication) that the highest grain densities are associated

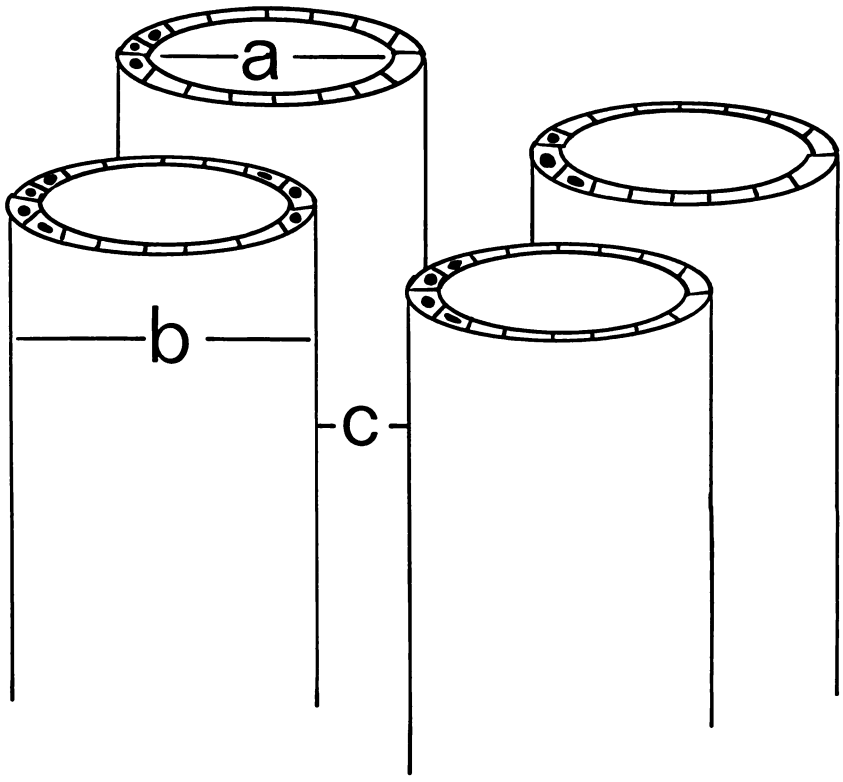

FIGURE 2
Simple tubular model of the histology of differentiated carcinoma of the colon used in the computer simulation. Calculations of the energy deposition to the nuclear volume fraction are performed for two cases: (A) sources distributed uniformly throughout the entire volume, and (B) sources placed on the outer wall of the tubule.

TABLE 6
Geometric Enhancement Factors for the Colon Model as a Function of the Mean Intertubular Distance*

Intertubular distance (μm)	Energy deposition per nucleus per decay (keV) (bound/unbound) ^{211}At Bragg curve	^{211}At Const. LET	^{131}I Const. LET
0	1.478	1.472	1.293
10	1.355	1.325	1.235
20	1.325	1.312	1.219
30	1.360	1.373	1.238
50	1.486	1.609	1.238
100	2.661	2.876	1.515
200	5.908	6.384	2.054

* The tubules are assumed cylinders with an outer radius of 50 μm and inner radius of 30 μm. The nuclei are centered 40 μm from the cylinder axis and have 5 μm radius. Antibody is assumed to bind uniformly to the outer surface of each tubule only.

with the close proximity of the outer cell surface. This demonstrates that in the clinical situation possible tumor cell nuclear dose enhancements may occur as a result of the close Ab localization to the tumor cell targets.

Recent in vitro cell survival assays by Kozak et al. (*44*) with anti-tac membrane affinic Ab labeled with the alpha-source bismuth-212 (^{212}Bi) have demonstrated that survival slopes can be arbitrarily steep when compared to studies with nonspecific Ab as a result of biasing the source to locations close to the target cells. The ratio of the D_0 values specific/non-specific Ab from the preceeding analysis is expected to be a function only of dilution of the cell assay. Very recent in vivo studies by Wessels et al. (*45*) have shown, that for comparable tumor doses measured with in situ TLD's, Ab targetted radionuclides may be more effective than acute and fractionated external beam exposures in reducing tumor growth. The effects measured in their study could be accounted for by the geometric dose enhancement discussed in this paper. However, Wessels et al. (*45*) also propose other possible mechanisms for the observed increase in radiotoxicity.

CONCLUSIONS

In order to assess the level of tumor cell sterilization from an administration of radiolabeled Ab one requires an accurate knowledge of the temporal and spatial variation of the source. Whereas this temporal data can be obtained in the tissue of tumor bearing animals by tissue removal and counting, for man this data must be obtained by immunoscintigraphic methods which at present are limited to only better than a centimeter resolution. Knowledge of the activity time course in tissue is needed to determine the cumulative activity, or more accurately cumulative energy release for heterogeneous source distributions—without which an accurate assessment of tissue dose is impossible.

The second aspect is the spatial distribution of the sources, which varies with time. The consequences of heterogeneity of radiolabeled Ab in tumor are (a) it may give rise to areas of low or zero Ab binding, so called "cold-regions", which may result in a considerable reduction in the dose compared with the equilibrium dose in such regions; and (b) if radiolabeled Ab either binds to the tumor cell membrane, or is internalized, then the energy deposition in the nuclei of those cells concerned can be markedly enhanced. The magnitude of geometric enhancement factors depends

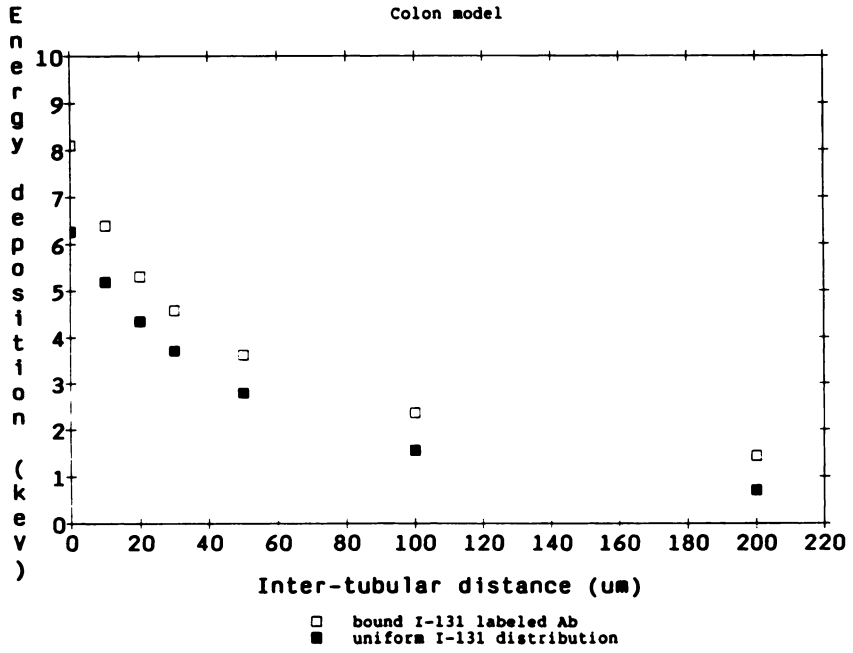

FIGURE 3
Mean energy deposition per nucleus per ^{131}I decay for: (A) sources placed uniformly throughout the tumor volume (■), and (B) attached to the outer wall of the tubules (□).

critically on the source to target nuclei relations at the micrometer level, and hence is very sensitive to the tumor histology, which sets out the spatial pattern of available antigen binding sites. The greatest enhancement factors occur for short range emitting radionuclides, especially alpha-sources. If alpha-radiolabeled Abs diffuse into tumor regions of low cellular density, e.g., in myxoid sarcomas and scirrhous carcinomas, then MIRD dose values could be inaccurate by an order of magnitude or greater. Experience with such tumors (Begent R., Boxer G.: private communication), suggests that the acellular areas of such tumors in man present major barriers to Ab penetration. The common pattern of Ab binding observed in animal models and patients is areas of isolated cells and acini, some heavily labeled, as seen from the grain pattern, others unlabeled. The evaluation of this problem is extremely complex and will require a detailed study of Ab localization from autoradiographs if a more accurate estimate of the tumor sterilizing effect of an administration of radiolabeled Ab is to be obtained.

ACKNOWLEDGMENTS

The authors thank Prof. K.D. Bagshawe F.R.S., Dr. R. Begent, and Dr. F. Searle of the CRC Laboratories, Charing Cross Hospital, London, and also Mrs. A. Harrison of the MRC Radiobiology Unit for useful discussions and ideas which have contributed greatly to the work presented in this paper.

One of the authors (JLH) would like to thank the Cancer Research Campaign who provided support for this project.

REFERENCES

1. Sitzmann JV, Order SE, Klein JL, Leichner PK, Fishman EK, Smith GW. Conversion by new treatment modalities of non-resectable to resectable hepatocellular cancer. *J Clin Oncol* 1987;5:1566–1573.
2. Lenhard RE, Order SE, Spunberg JJ, Asbell SO, Leibel SA. Isotopic immunoglobulin: a new systemic therapy for advanced Hodgkin's disease. *J Clin Oncol* 1985;3:1296–1300.
3. Order SE, Klein JL, Ettinger D, Alderson P, Siegelman S, Leichner P. Use of isotopic immunoglobulin in therapy. *Cancer Res* 1980;40:3001–3007.
4. Tuttle SE, Jewell SD, Mojzisik CM, et al. Intraoperative radioimmunolocalization of colorectal carcinoma with a hand-held gamma probe and Mab B72.3 comparison of in vivo gamma probe counts with in vitro Mab radiolocalization. *Int J Cancer* 1988;42:352–358.
5. Sedlacek HH, Schulz G, Steinstraesser A, et al. Monoclonal antibodies in tumour therapy. *Contributions to oncology.* Vol. 32. Basel: Kerger, 1988:68–80.
6. Shawler DL, Bartholomew RM, Smith LM, Dillman RO. Human immune response to multiple injections of murine IgG. *J Immunol* 1985;135:1530–1535.
7. Klein JL, Sandoz JW, Kopher KA, Leichner PK, Order SE. Detection of specific antibodies in patients treated with radiolabeled antibody. *Int J Radiat Biol* 1986;12:939–943.
8. Jain RK, Baxter LT. Mechanisms of heterogeneous distribution of monoclonal antibodies and other macromolecules in tumors: significance of elevated interstitial pressure. *Cancer Res* 1988;48:7022–7032.
9. Cobb LM. Intratumour factors influencing access of antibody to tumour cells. *Cancer Immunol Immunother* 1989;28:235–240.
10. Edwards PAW. Heterogeneous expression of cell-surface antigens in normal epithelia and their tumours, revealed by monoclonal antibodies. *Br J Cancer* 1985;51:149–160.
11. Enblad P, Glimelius B, Busch C, Ponten J, Pahlman L. Antigenic heterogeneity in adeno carcinomas of the rectum and their secondaries. *Br J Cancer* 1987;55:503–508.
12. Ludatsher RM, Gellei B, Barzilai D. Ultrastructural observations on the capillaries of human thyroid tumours. *J Pathol* 1979;128:57–62.
13. Cobb LM, Humphreys JA, Harrison A. The diffusion of a tumour-specific monoclonal antibody in lymphoma infiltrated spleen. *Br J Cancer* 1987;55:53–55.
14. Porter EH, Hewitt HB, Blake ER. Transplantation kinetics of tumour cells. *Br J Cancer* 1973;27:55–62.
15. Hamburger AW, Salmon SE. Primary bioassay of human tumour cells. *Science* 1977;197:461–463.
16. Order SE, Klein JL, Ettinger D, et al. Phase I-II study of radiolabeled antibody integrated in the treatment of primary hepatic malignancies. *Int J Radiat Oncol Biol Phys* 1980;6:703–710.
17. DeNardo GL, Raventos A, Hines HH. Requirements for a treatment planning system for radioimmunotherapy. *Int J Radiat Oncol Biol Phys* 1985;11:335–348.
18. Carrasquillo JA, Krohn KA, Beaumier P, et al. Diagnosis of and therapy for solid tumors with radiolabeled antibodies and immune fragments. *Cancer Treat Rep* 1984;68,1:317–328.
19. Ledermann JA, Begent RHJ, Bagshawe KD, Riggs SJ, Searle F, Glaser MG. Repeated antitumour antibody therapy in man with suppression of the host response by cyclosporin A. *Br J Cancer* 1988;58:654–657.
20. Stewart JS, Hird V, Snook D, Sullivan M, Myers MJ, Epenetos A. Intraperitoneal ^{131}I and ^{90}Y-labelled monoclonal antibodies for ovarian cancer: pharmacokinetics and normal tissue dosimetry. *Int J Cancer Suppl* 1988;3:71–76.
21. Order SE, Klein JL, Leichner PK, Frincke J, Lollo C, Carlo DJ. ^{90}Yttrium antiferritin—a new therapeutic radiolabeled antibody. *Int J Radiat Oncol Biol Phys* 1986;12:277–281.
22. Hnatowich DJ, Chinol M, Gionet M, et al. Therapy trials of yttrium-90 labeled anti-tumor antibodies [Abstract]. *J Nucl Med* 1988;29(suppl):846.
23. Harrison A, Royle L. Efficacy of astatine-211-labeled monoclonal antibody in treatment of murine T-cell lymphoma. *NCI Monogr* 1987;3:157–158.
24. ICRU Report 32: Methods of assessment of absorbed dose in clinical use of radionuclides. 1979; Washington D.C., International Commission on Radiation Units and Measurements.
25. Snyder WS, Ford MR, Warner GG, Fisher HL. Estimates of absorbed fractions for monoenergetic photon sources uniformly distributed in various organs of a heterogeneous phantom. MIRD Pamphlet No. 5. *J Nucl Med* 1969;10(suppl 3)5–52.
26. ICRP Publication 2. Recommendations of the International Commission on Radiation protection. Oxford, Pergamon Press, 1959.
27. ICRP Publication 23. Report of the Task Group on Reference Man. Oxford, Pergamon Press, 1975.
28. Snyder WS, Ford MR, Warner GG, Watson SB. "S," Absorbed dose per unit cumulated activity for selected radionuclides and organs. *MIRD Pamphlet No. 11.* New York: Society of Nuclear Medicine, 1975.
29. Dillman LT, Von der Lage. Radionuclide decay schemes and nuclear parameters for use in radiation dose estimation. *MIRD Pamphlet No. 10.* New York: Society of Nuclear

Medicine, 1975.
30. Humm JL. Dosimetric aspects of radiolabeled antibodies for tumor therapy. *J Nucl Med* 1986;27:1490–1497.
31. Kwok CS, Prestwich WV, Wilson BC. Calculation of radiation doses for nonuniformly distributed β and γ radionuclides in soft tissue. *Med Phys* 1985;12:405–412.
32. Howell RW, Rao DV, Sastry KSR. Macroscopic dosimetry for radioimmunotherapy: Nonuniform activity distributions in solid tumors. *Med Phys* 1989;16,1:66–74.
33. Jungermann JA, Yu KP, Zanelli CI. Radiation absorbed dose estimates at the cellular level for some electron-emitting radionuclides for radioimmunotherapy. *Int J Appl Isot* 1984;35: 883–888.
34. Wessels BW, Griffith MH, Bradley EW, et al. Dosimetric measurements and radiobiological consequences of radioimmunotherapy in tumor bearing mice. Fourth International Radiopharmaceutical Dosimetry Symposium, CONF-851113:446–457, Oak Ridge, 1985.
35. Griffith MH, Yorke ED, Wessels BW, DeNardo GL, Neacy WP. Direct dose confirmation of quantitative autoradiography with micro-TLD measurements for radioimmunotherapy. *J Nucl Med* 1988;29:1795–1809.
36. Fisher DR. The microdosimetry of monoclonal antibodies labeled with alpha particles. Fourth International Radiopharmaceutical Dosimetry Symposium, CONF-851113:446–457, Oak Ridge, 1985.
37. Barendsen GW. Impairment of the proliferative capacity of human cells in culture by α-particles with differing linear-energy transfer. *Int J Radiat Biol* 1964;8:453–466.
38. Thacker J, Stretch A, Stevens MA. Mutation and inactivation of cultured mammalian cells exposed to beams of accelerated heavy ions II. Chinese hamster V79 cells. *Int J Radiat Biol* 1979;36:137–148.
39. Hall E. Radiobiology for the radiologist. Third edition. Philadelphia: J.B. Lippincott Company, 1988.
40. Gabel D, Foster S, Fairchild RG. The Monte Carlo simulation of the biological effect of the $^{10}B(n,\alpha)^{7}Li$ reaction in cells and tissue and its implication for boron capture therapy. *Radiat Res* 1987;111:14–25.
41. Humm JL. A microdosimetric model of astatine-211 labeled antibodies for radioimmunotherapy. *Int J Radiat Oncol Biol Phys* 1987;13:1767–1773.
42. Walsh PJ. Stopping power and range of alpha particles. *Health Phys* 1970;19:312–313.
43. Mach JP, Buchegger F, Formi M, et al. Use of radiolabelled monoclonal anti-CEA antibodies for the detection of human carcinomas by external photoscanning and tomoscintigraphy. *Immunol Today* 1981;2:239–249.
44. Kozak RW, Atcher RW, Gansow O, et al. Bismuth-212-labeled anti-tac monoclonal antibody: α-particle-emitting radionuclides as modalities for radioimmunotherapy. *Proc Natl Acad Sci USA* 1986;83:474–478.
45. Wessels BW, Vessella RL, Palme DF, Berkopec JM, Smith GK, Bradley EW. Radiobiological comparison of external beam irradiation and radioimmunotherapy in renal cell carcinoma xenografts. *Int J Radiat Oncol Biol Phys* 1989; 17:6.